

CLASSICAL TRAJECTORY STUDIES OF KEV  
IONS INTERACTING WITH SOLID SURFACES

Barbara J. Garrison\*

Department of Chemistry  
The Pennsylvania State University  
University Park, PA 16802

I. INTRODUCTION

Classical dynamics has been used extensively over the past twenty years to aid in our microscopic understanding of chemical reactions and properties of matter. As our experience has grown, the complexity of the systems studied has expanded from simple atom-diatom collisions<sup>1,2</sup> and hard sphere liquids<sup>3</sup> to more complicated gas-phase reactants (see the chapters by Schatz and Elgersma in this book) and more realistic liquids.<sup>4</sup> Dynamics calculations allow the determination of average experimental quantities, and at the same time, they give physical insight into the microscopic mechanisms. Results of the calculations are very visual, allowing one to picture the motion of particles. The variety of applications of classical dynamics in chemistry is evidenced by the contributions to this volume.

We have been using the classical trajectory method as an approach to investigate the interaction of high-energy ions with solids. The bombardment of a solid by ions in the energy range 200-5000 eV causes particles to eject from the surface, a phenomenon which is often called sputtering. This ejection of particles may be a desired effect such as in secondary ion mass spectrometry (SIMS) where the nature of the ejected particles reveals something of the original configuration of the surface. On the other hand, neutral particles ejected from the walls of the chamber in a tokamak, a device for controlling nuclear fusion, cause a deleterious cooling effect. Our goal is to understand the overall ion bombardment process. In particular, we are interested in which experimental observables might be

\*Alfred P. Sloan Research Fellow

used to measure structural parameters (bond lengths and angles) of atoms adsorbed on surfaces.

As for all scattering calculations, an interaction potential among the atoms in the system to be investigated is needed. In most of our calculations there are 2 to 4 different types of atoms with a total of 250 to 400 atoms. A potential surface for a system of this size is not known. Yet, to date, using simply a pairwise additive form, we have been able to understand, explain, and predict many experimental observables. How is this possible? In this ion bombardment process, energetic collisions play an important role. These collisions mainly sample the repulsive wall of the interaction potential. Physically this wall is an indication of the presence of an atom. It turns out that many observables are strongly influenced by the arrangement of atoms in the solid. Other observables naturally are sensitive to the details of the interaction potential. Thus, despite the complexity of the system, the classical dynamics method, using simple model potentials, can be very useful in helping to understand the ion bombardment process.

In section II a brief description of the method will be given. Emphasis will be placed on the differences from thermal-energy gas-phase atom-molecule collision dynamics. In addition the types of observables and systems studied to date will be delineated. In section III we will discuss the sensitivity of the total yield, cluster formation, and angular distributions to interaction potential. In general we find that absolute yields are difficult to accurately calculate but relative yields which can be directly compared to experiment can be determined.

## II. METHOD

The dissipation of the momentum of the primary ion into the solid is modeled using classical dynamics. The infinite solid is approximated by a microcrystallite with or without adsorbate atoms or molecules. The positions and momenta of the primary ion, all lattice atoms, and adsorbates are developed in time by numerically integrating Hamilton's equations of motion. The final positions and momenta of the ejected particles can then be used to determine yields, energy distributions, angular distributions, and possible cluster formation.<sup>5-9</sup>

Since a crystallite of finite size is being used to approximate an infinite system, care must be taken to avoid spurious results due to the edges of the crystallite. Considerable testing has been performed for ion impacts on various sized crystallites in order to assure that the great majority (about 95%) of the ejection events of the infinite solid are described by the final choice of the number of atoms. We have found that for 600 eV Ar<sup>+</sup> ion impact at normal

incidence on clean metals, 4 layers of about 60 atoms per layer are sufficient.<sup>6</sup> Testing at higher ion energies indicates that increasing the surface size (atoms/layer) is more important than increasing the number of layers.

The determination of the initial positions and momenta of the ion and atoms in the solid is straightforward. Because experimental data to date have not shown any significant temperature effects, the atoms in the crystal are assumed to be initially at their equilibrium positions with no momentum. Depending on the system of interest, different crystal faces can be oriented toward the incoming ion. Since in SIMS experiments the velocity, direction, and mass of the primary ion can be selected, the impact point of the primary ion on the surface is the only initial condition left to be averaged. To obtain quantities comparable to experiment, the ion must strike at various points within a surface impact zone that represents the symmetry of the exposed crystal face and possible overlayer structure.<sup>6,10</sup> The number of impact points that are necessary depends on the observable of interest. For total yields, often 50-100 ion trajectories are sufficient. For angular distributions of dimers, as many as 1300 impact points may be necessary. This is in contrast to gas-phase trajectory calculations, where often thousands of trajectories are sampled because very few of them result in the desired outcome. Generally, all the ion impacts give rise to the ejection of at least a few particles, resulting in a relatively smaller number of needed trajectories.

In contrast to gas-phase classical trajectory calculations, the forces in this system vary rapidly with distance. As a consequence, no computer time advantage is gained by using a high-order predictor-corrector integrator. A low-order predictor-corrector is most efficient computationally.<sup>11,12</sup> One impact point on a clean metal system with 240 atoms typically takes 120 timesteps, integrates for  $2 \times 10^{-13}$  seconds and takes about 30 seconds on a CDC 7600 computer. The computer time is approximately proportional to  $N^2$  where  $N$  is the number of atoms in the system.

The integration is terminated when it is physically impossible for more particles to eject. Operationally, this condition occurs when the most energetic atom remaining in the solid has about 2 eV of kinetic energy. This termination energy is lower for adsorbates which have smaller surface binding energies.

Due to the complexity of the system we have chosen to use an interaction potential which is pairwise additive between the particles. For the mutual interaction of atoms within the solid system, the pair potential includes a repulsive part at short range splined to a long range attraction. For an internuclear separation  $R$  the atom-atom pair potential in the solid has the general form

$$V = Ae^{-BR} \quad R \leq R_a \quad (1a)$$

$$V = C_0 + C_1R + C_2R^2 + C_3R^3 \quad R_a < R < R_b \quad (1b)$$

$$V = D_e e^{-\beta(R-R_e)} (e^{-\beta(R-R_e)} - 2) \quad R_b \leq R \leq R_c \quad (1c)$$

$$V = 0 \quad R > R_c \quad (1d)$$

The interaction of the ion with the other species is assumed to be repulsive with the form

$$V = Ae^{-BR} \quad R \leq R_a \quad (2a)$$

$$V = 0 \quad R > R_a \quad (2b)$$

Whenever possible the parameters are chosen to fit experimental data. The parameters actually used in the calculations of each system are given in the publication of the respective work.

In order to examine structural effects we must place atoms in arbitrary positions, for example, atomic adsorbates in linear bonded and fourfold bridge sites on a (001) crystal face. This is contrary to the use of pair potentials which imply a single lowest energy site. The collision time of the total cascade is so short (about 0.2 ps), however, that the atoms do not have time to thermally relax to their equilibrium positions. The pair potentials for the nearest neighbor atoms must, though, have realistic equilibrium separations. This allows us to examine larger systems without worrying about the low-energy intricacies of the interaction potential.

Many properties can be calculated from the final positions and momenta of the particles which eject. These include yield (average number of particles which eject per incident ion), cluster formation probabilities, energy distributions, and angular distributions. One could also inspect vibrational and rotational state distributions of the ejected particles, although this property is more dependent on the interaction potential. In addition, the final energy and scattering angles of the primary ion can be monitored as in ion scattering experiments.<sup>13</sup>

Besides determining the experimental observables, the classical dynamics procedure allows us to examine other properties, most notably mechanisms. We can examine how the atoms eject, what the original configuration of the atoms was that resulted in a cluster, how the cluster formed, and which atoms eject at specific angles.

Table 1  
Ejection yield of 600 eV Ar<sup>+</sup> on copper (001), (110), and (111).

Crystal face	Calculated yield	Relative yield <sup>a</sup>			
		Calculated	Experimental		
		Cu	Cu <sup>b</sup>	Ag <sup>b</sup>	Au <sup>c</sup>
(001)	4.06	1.0	1.0	1.0	1.0
(110)	3.54	0.9	0.6	0.7	0.7
(111)	6.50	1.6	1.8	1.6	1.5

a. relative to the (001) face

b. measured at 2 keV by weight loss (reference 19)

c. measured at 2 keV by weight loss (reference 20)

Many systems have been examined using this procedure. The initial system studied extensively by Harrison and coworkers is copper bombarded by Ar<sup>+</sup> ions.<sup>5,11</sup> Since that time we have concentrated on the low-index faces of the fcc metals copper and nickel.<sup>5,7,8,12</sup> In addition, adsorbates such as atomic oxygen,<sup>10</sup> carbon monoxide,<sup>14</sup> and benzene<sup>15</sup> have been included in the calculations. Preliminary studies of alloys have also been completed.<sup>16</sup> Similar studies on a two-dimensional alkali halide crystal have been performed by Heyes, Barber, and Clarke.<sup>17</sup>

### III. DISCUSSION

The future of using this classical dynamics procedure to understand and explain ion bombardment experiments will lie in our ability to know which observables can be calculated reliably and which are overly sensitive to the interaction potential. In the following discussion, specific observables will be discussed separately.

#### A. Total Yields

The absolute yield or average number of particles to eject per incident ion is computationally the easiest observable to determine. However, it is difficult to calculate the yield accurately since it is very sensitive to the interaction potential. We have been successful, though, in determining relative yields. For example, among the low-index faces of copper, the ratios of yields are rather insensitive to the interaction potential. In Table 1 are the results of

a study of 600 eV  $\text{Ar}^+$  ions bombarding the three low-index faces of copper.<sup>6,18</sup> The calculated absolute yields are about a factor of two higher than the experimental ones.<sup>19,20</sup> The calculated relative yields among the three crystal faces are, however, in quite good agreement with experiment. In fact, the relative yields for the three fcc metals Cu, Ag, and Au are so similar that one can conclude that the arrangement of atoms in the (111) face is responsible for the higher yield relative to the (001) face. This is shown even more dramatically in a study by Harrison where he varied the parameters in the exponential repulsion pair potential of equation (2a) for the interaction between the  $\text{Ar}^+$  and Cu.<sup>21</sup> In this study the  $\text{Ar}^+$  ion has 5 keV of energy, and Harrison was examining only the (111) and (001) faces. In one part of the study the A parameter of equation (2a) was fixed at 71.30 keV and the range parameter B was varied. In Fig. 1a are the calculated yields for these potentials for both the (111) and (001) faces. The yields vary by a factor of 6. The ratio of the

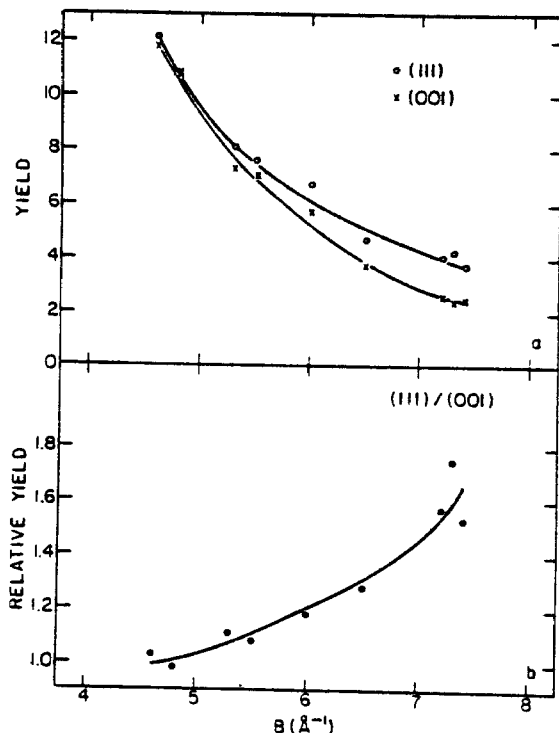


Fig. 1. Ejection yields. Average number of Cu atoms which eject per incident  $\text{Ar}^+$  ion versus the range parameter B of the Ar-Cu<sup>+</sup> interaction potential. (a) Absolute yields for the (111) and (001) faces. (b) Ratio of the yield from the (111) face to the yield from the (001) face.

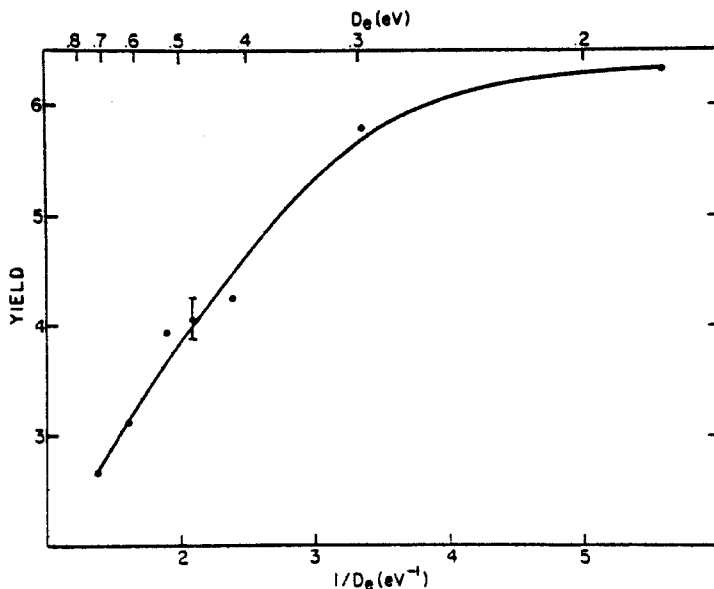


Fig. 2. Ejection yield versus well depth,  $D_e$ , of the Cu-Cu pair potential.

yield from the (111) face to that from the (001) face, as shown in Fig. 1b, only varies by 60 percent with the (111) face generally giving a higher yield.

The parameters in the substrate pair potential [equation (1c)] used to describe a system such as copper metal are often fit to bulk properties such as sublimation energies and compressibilities.<sup>22</sup> For copper, this procedure results in a well depth of 0.48 eV. Gas phase  $\text{Cu}_2$ , however, is bound by 2.05 eV,<sup>23</sup> a factor of four larger. Undoubtedly as an atom starts to eject, the appropriate interaction is not that of the bulk pair potential. Shown in Fig. 2 is the yield of particles ejected versus the Cu-Cu pair potential well depth,  $D_e$ . The primary ion is  $\text{Ar}^+$  which strikes the Cu(001) crystal face at normal incidence with 600 eV of energy. The yield depends on  $D_e$ . Using the incorrect value of  $D_e$  or even using pair potentials when they are not appropriate can, thus, cause significant variations in the total yield.

In summary, the absolute yield of particles ejected is a very difficult quantity to calculate due to the large dependence on potential parameters. In addition, there are inelastic effects which will also hinder our ability to correctly predict absolute yields. We can, however, determine relative yields, for example, between various crystal faces of the same metal,<sup>6,18</sup> as a function of the energy of

Table 2  
Relative cluster yields.<sup>a</sup>

Ratio	Crystal face	
	(001)	(111)
$\text{Cu}_2/\text{Cu}$	1.0 (37/765) <sup>c</sup>	2.3 (107/953)
$\text{Ni}_2^+/\text{Ni}^+{}^b$	1.0	1.8
$\text{Cu}_3/\text{Cu}$	1.0 (6/765)	1.9 (14/953)
$\text{Ni}_3^+/\text{Ni}^+{}^b$	1.0	6.3

a. normalized to the (001) face

b. from reference 25

c. The absolute number calculated for each species is given in the parentheses.

the primary ion,<sup>21</sup> as a function of the angle of incidence of the primary ion<sup>5,12</sup> or as a function of coverage of an adsorbate.<sup>10</sup>

### B. Cluster Formation

Many workers have hoped that the composition of the clusters of atoms that eject during ion bombardment could be directly interpreted as a local configuration of atoms in the solid. The molecular dynamics procedure is an ideal method with which to examine cluster formation, since we can analyze the motion of the individual atoms. The calculations have shown that metal clusters and metal-adsorbate clusters form by a recombination mechanism. That is, the atoms in the cluster do not necessarily originate from nearest neighbor sites on the surface.<sup>7,8,10,12,24</sup> They do originate, however, from a fairly localized region of the surface because they must eject near enough to each other to experience attractive binding interactions. Molecular adsorbates, such as carbon monoxide<sup>14</sup> or benzene<sup>15</sup> can, however, eject intact.

The ability to calculate absolute cluster yields suffers from all the same problems (discussed in section III.A) as calculating absolute total yields. We can, however, calculate relative cluster yields. Table 2 gives the calculated relative cluster yields for the three low-index faces of an fcc metal.<sup>8,18</sup> Also given are experimental SIMS measurements.<sup>25</sup> Two ratios have been taken. First, we divide the cluster yield by the monomer yield. Hopefully, this



removes some of the uncertainty about the ionization process. Second, we normalize the cluster/monomer ratios to the value from the (001) face. There is qualitative agreement between the experiments and the calculations, particularly for the dimer yields. There are poor statistics in both the calculation and experiment for the trimer yields, thus less significance can be attributed to the comparison with experiment.

### C. Angular Distributions

The observable that appears to contain the most structural information is the angular distribution of the ejected particles. The angular distributions of metal atoms ejected from solids have been known since the 1960's to reflect the symmetry of the crystal face.<sup>26</sup> The molecular dynamics calculations have predicted that the angular distributions of the adsorbates will depend not only on the symmetry of the crystal face but also on their bonding site and their height above the surface.<sup>9,27</sup> We have hopes of being able to measure bond lengths and angles by detailed experimental measurements of the angular distributions.

To eventually make experimental determinations of structural parameters, we must know the major factors influencing the ejection angles of the particles. Does the relative placement of atoms on the surface control the angles of ejection of the atom, or do other features in the interaction potential dominate this process? The system we have chosen to investigate is oxygen adsorbed atomically in a  $c(2 \times 2)$  (half monolayer) overlayer on Ni(001).<sup>28</sup> Low-energy electron diffraction (LEED) studies have indicated that the oxygen is 0.9 Å above the surface, presumably in a fourfold bridge bonded site (Fig. 3a).<sup>29</sup> We have recently performed an extensive series of calculations where the site, height, and interaction potential of the oxygen atoms are varied.<sup>30</sup>

For a constant interaction potential, we find that the angular distributions of the ejected oxygen atoms are sensitive to both the adsorption site and the height above the surface. The most striking variation is with bonding site. The height variation is more subtle and more dependent on potential. Figs. 3a,b show the placement of oxygen atoms in a  $c(2 \times 2)$  overlayer for a fourfold bridge site and an atop or linear bonded site. Figs. 3c-f display angular distributions of the ejected oxygen atoms with greater than 10 eV of kinetic energy. The angular distributions are displayed on a flat plate collector a large distance above the surface. The radial distance is proportional to the tangent of the polar angle of ejection. The azimuthal orientation is the same as that in frames a and b.

For the Ni-O interaction, a Morse potential, [equation (1c)], was used for all internuclear separations. In the calculations

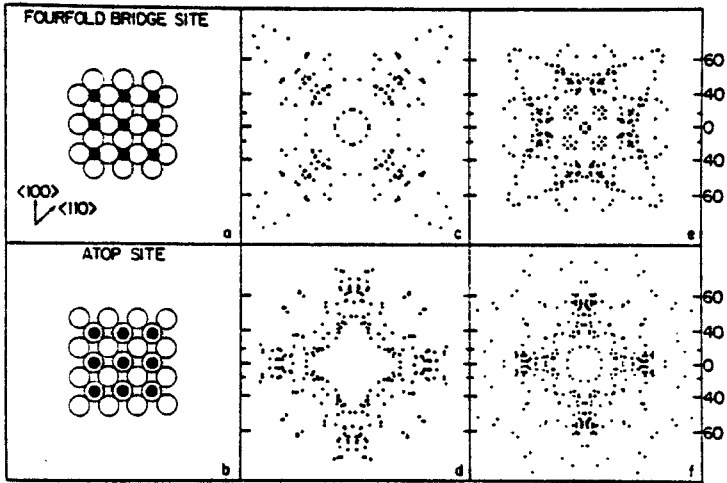


Fig. 3. Angular distributions of ejected oxygen atoms. (a)  $c(2 \times 2)$  overlayer of oxygen atoms in fourfold bridge sites on Ni(001). (b)  $c(2 \times 2)$  overlayer of oxygen atoms in atop or linear bonded sites on Ni(001). (c-f) Only the angular distributions of oxygen atoms with greater than 10 eV of kinetic energy are shown: (c) Fourfold bridge site,  $\beta = 2.0 \text{ \AA}^{-1}$ . (d) Atop site,  $\beta = 2.0 \text{ \AA}^{-1}$ . (e) Fourfold bridge site,  $\beta = 2.45 \text{ \AA}^{-1}$ . (f) Atop site,  $\beta = 2.45 \text{ \AA}^{-1}$ .

presented here for the oxygen atoms in fourfold bridge sites, values of the parameters are  $D_e = 0.18 \text{ eV}$  and  $R_e = 2.0 \text{ \AA}$  with  $\beta = 2.0 \text{ \AA}^{-1}$  and  $2.45 \text{ \AA}^{-1}$  for the distributions in Figs. 3c and 3e, respectively. To maintain the same binding energy of the oxygen atoms to the surface, for the atop site calculations a value of  $D_e = 0.53$  was used. Again  $R_e$  was  $2.0 \text{ \AA}$ , and the calculations were done with  $\beta = 2.0 \text{ \AA}^{-1}$  and  $2.45 \text{ \AA}^{-1}$  for Figs. 3d and 3f, respectively.

All the atop distributions, Figs. 3d and 3f, are characterized by a region of high intensity in the  $\langle 100 \rangle$  directions (vertical and horizontal directions). The direction of ejection is the same as for the substrate Ni atoms.<sup>9,27,28</sup> This characteristic pattern arises from the distinctive alignment of the oxygen atoms which are in the path of the ejecting substrate atoms. Changing the height of the adsorbate atom or the interaction potential causes the polar angle of the ejection to vary but does not alter the azimuthal direction. The angular distributions of the oxygen atoms ejected from fourfold bridge sites, Figs. 3c and 3e, have their maximum intensity rotated from the  $\langle 100 \rangle$  azimuths. Again the local geometry controls the ejection direction, although the mechanism is more complicated than for the atop site case. The angular distributions of oxygen atoms ejected from fourfold sites are distinct from the distributions of oxygen atoms from atop sites.

It is a little premature to make any definite conclusion regarding our ability to measure structural parameters of adsorbates on surfaces. The necessary high-resolution experiments are only beginning to become available.<sup>31</sup> However, we currently feel that to extract bonding site information from the angular distributions of ejected particles is possible but that determination of adsorbate height will be more difficult due to the greater sensitivity to the interaction potential. If this hypothesis continues to be valid, angle-resolved SIMS then would be complementary to LEED, as LEED experiments can more reliably determine the height of an adsorbate than the site geometry.

#### IV. FUTURE DIRECTIONS

The classical dynamics procedure discussed here has been quite successful in helping us understand, explain, and predict many of the results from ion bombardment experiments. We are at the stage where detailed information is needed from experiments so that we can refine various assumptions in the model, most notably the uncertainty in the potential parameters. Currently angle-resolved SIMS experiments which are measuring highly resolved energy and angular distributions of ejected particles are underway at Penn State under the direction of N. Winograd. These experiments will enable us to make very detailed comparisons with the calculations. One major obstacle remaining is that SIMS experiments measure ion intensities while the dynamics calculations follow the motion of all particles, most of which are neutral. Undoubtedly, these experiments will also be the driving force for the inclusion of ionization processes in the model of the particle-ejection process.

#### V. ACKNOWLEDGMENTS

These ideas have developed over the past few years due to the interaction with exceptional collaborators. These people include Professors Nicholas Winograd and Don Harrison, Jr., Dr. Shukla Kapur, and graduate students Karin Foley, Steven Holland, and Richard Gibbs. Support is acknowledged from the Camille and Henry Dreyfus Foundation for a grant for newly appointed young faculty, the Alfred P. Sloan Foundation for a Research Fellowship, the Research Corporation for a Cottrell grant, and The Pennsylvania State University for a Research Initiation grant. Portions of the computations were supported by the National Resource for Computation in Chemistry under a grant from the National Science Foundation and the U.S. Department of Energy (Contract No. W-7405-ENG-48).

## VI. REFERENCES

1. (a) F. T. Wall, L. A. Hiller, Jr., and J. Mazur, Statistical computation of reaction probabilities, *J. Chem. Phys.* 29: 255 (1958); (b) F. T. Wall, L. A. Hiller, Jr., and J. Mazur, Statistical computation of reaction probabilities, II, *J. Chem. Phys.* 35: 1284 (1961); (c) D. L. Bunker, Monte Carlo calculations of triatomic dissociation rates. I.  $N_2O$  and  $O_3$ , *J. Chem. Phys.* 37: 393 (1962); (d) J. C. Keck, Statistical investigation of dissociation cross-sections for diatoms, *Disc. Faraday Soc.* 33: 173 (1962); (e) N. C. Blais and D. L. Bunker, Monte Carlo calculations. III. A general study of biomolecular exchange reactions, *J. Chem. Phys.* 39: 315 (1963).
2. See also, for example, D. G. Truhlar and J. T. Muckerman, Reactive scattering cross sections: Quasiclassical and semiclassical methods, in: "Atom-Molecule Collision Theory: A Guide for the Experimentalist", R. B. Bernstein, ed., Plenum Press, New York (1979), p. 505.
3. B. J. Adler and T. E. Wainwright, Studies in molecular dynamics. I. General method, *J. Chem. Phys.* 31: 459 (1959).
4. See, for example, "Computer Modeling of Matter", P. Lykos, ed., ACS Symposium Series, No. 86, Washington, D.C. (1978).
5. D. E. Harrison, Jr., W. L. Moore, Jr., and H. T. Holcombe, Computer simulation of sputtering II, *Rad. Eff.* 17: 167 (1973).
6. D. E. Harrison, Jr., P. W. Kelly, B. J. Garrison, and N. Winograd, Low energy ion impact phenomena on single crystal surfaces, *Surface Sci.* 76: 311 (1978).
7. B. J. Garrison, N. Winograd, and D. E. Harrison, Jr., Formation of small metal clusters by ion bombardment of single crystal surfaces, *J. Chem. Phys.* 69: 1440 (1978).
8. N. Winograd, D. E. Harrison, Jr., and B. J. Garrison, Structure sensitive factors in the ion bombardment of single crystal surfaces, *Surface Sci.* 78: 467 (1978).
9. N. Winograd, B. J. Garrison, and D. E. Harrison, Jr., Angular distributions of ejected particles from ion bombarded clean and reacted single crystal surfaces, *Phys. Rev. Lett.* 41: 1120 (1978).
10. B. J. Garrison, N. Winograd, and D. E. Harrison, Jr., Atomic and molecular ejection from ion bombarded reacted single crystal surfaces, *Phys. Rev. B* 18: 6000 (1978).
11. D. E. Harrison, Jr., W. L. Gay, and H. M. Effron, Algorithm for the calculation of the classical equations of motion of an N-body system, *J. Math. Phys.* 10: 1179 (1969).
12. K. E. Foley and B. J. Garrison, Mechanisms of particle ejection from Cu(001) induced by directional orientation of the bombarding primary ion, *J. Chem. Phys.* 72: 1018 (1980).
13. B. J. Garrison, Theory of ion scattering from single crystals, *Surface Sci.* 87: 683 (1979).

14. N. Winograd, B. J. Garrison, and D. E. Harrison, Jr., Mechanisms of CO ejection from ion bombarded single crystal surfaces, *J. Chem. Phys.* 73: 3473 (1980).
15. B. J. Garrison, Mechanisms of ejection of organic molecules from surfaces by keV ion bombardment, *J. Amer. Chem. Soc.* 102: 6553 (1980).
16. B. J. Garrison, manuscript in preparation.
17. D. M. Heyes, M. Barber, and J. H. R. Clarke, The use of sputtering as a method for analyzing surface chemical compositions: A molecular dynamics study, First International Meeting on SIMS, Muenster, Germany, September 1977.
18. N. Winograd, B. J. Garrison, T. Fleisch, W. N. Delgass, and D. E. Harrison, Jr., Structure sensitive factors in molecular cluster ejection by ion bombardment of Ni single crystals reacted with CO and O<sub>2</sub>, *J. Vac. Sci. Tech.* 16: 629 (1979).
19. G. D. Magnuson and C. E. Carlston, Sputtering yield of single crystals bombarded by 1- to 10-keV ions, *J. Appl. Phys.* 34: 3267 (1963).
20. M. T. Robinson and A. L. Southern, Sputtering experiments with 1- to 5-keV Ar<sup>+</sup> ions. II. Monocrystalline targets of Al, Cu, and Au, *J. Appl. Phys.* 38: 2969 (1967).
21. D. E. Harrison, Jr., Full lattice simulation of atom ejection mechanisms and sputtering, in: "Proceedings of the Symposium on Sputtering, Perchtoldsdorf-Wien, Austria, April 28-30, 1980", P. Varge, G. Betz, and F. P. Viebock, eds., Institut für Allgemein Technische Universität Wien, Austria.
22. A. Anderman, AFCRL-66-688 Atomic International, Canoga Park, CA, unpublished. Taken from reference 5.
23. B. Rosen, "International Tables of Selected Constants", Pergamon Press, New York (1970).
24. D. E. Harrison, Jr. and C. B. Delaplain, Computer simulation of the sputterings of clusters, *J. Appl. Phys.* 47: 2242 (1976).
25. M. Barber, R. S. Bardoli, J. C. Vickerman, and J. Wolstenholme, SIMS study of adsorption on Ni(110), (100), and (111), in: "Proceedings of the 7th International Vacuum Congress and 3rd International Conference on Solid Surfaces", R. Dobrozemsky, ed., F. Berger und Söhne, Vienna (1977), p. 983.
26. For a good review of this topic, see G. Carter and J. S. Colligan, "Ion Bombardment of Solids", American Elsevier, New York (1968).
27. S. P. Holland, B. J. Garrison, and N. Winograd, Surface structure from angle-resolved SIMS: Oxygen on Cu(001), *Phys. Rev. Lett.* 43: 220 (1979).
28. S. P. Holland, B. J. Garrison, and N. Winograd, Azimuthal anisotropies of dimer ions ejected from ion bombarded Ni(001), *Phys. Rev. Lett.* 44: 756 (1980).
29. M. van Hove and S. Y. Tong, Chemisorption bond lengths of chalcogen overlayers at a low coverage by convergent perturbation methods, *J. Vac. Sci. Tech.* 12: 230 (1975).

30. S. Kapur and B. J. Garrison, Theoretical studies of the angular distributions of oxygen atoms ejected from an ion bombarded  $c(2 \times 2)$  overlayer of oxygen on Ni(001): I. Effect of geometry and II. Effect of potential, manuscripts in preparation.
31. R. A. Gibbs and N. Winograd, private communication.